ELSEVIER

Journal of Alloys and Compounds 446–447 (2007) 504–507

Journal of ALLOYS AND COMPOUNDS

www.elsevier.com/locate/jallcom

Neutron vibrational spectroscopy of the Pr_2Fe_{17}-based hydrides

T.J. Udovic [a,*], W. Zhou [a,b], H. Wu [a,c], C.M. Brown [a,d], J.J. Rush [a,c], T. Yildirim [a,b], E. Mamontov [a,c,1], O. Isnard [e,f]

[a] *NIST Center for Neutron Research, National Institute of Standards and Technology, 100 Bureau Drive, MS 8562, Gaithersburg, MD 20899-8562, USA*
[b] *Department of Materials Science and Engineering, University of Pennsylvania, 3231 Walnut St., Philadelphia, PA 19104-6272, USA*
[c] *Department of Materials Science and Engineering, University of Maryland, College Park, MD 20742-2115, USA*
[d] *Indiana University Cyclotron Facility, 2401 Milo B. Sampson Lane, Bloomington, IN 47408, USA*
[e] *Laboratoire de Cristallographie, CNRS, associé à l'Université J. Fourier, BP 166X, F-38042 Grenoble Cedex, France*
[f] *Institut Universitaire de France, Maison des Universités, 103 Boulevard Saint-Michel, F-75005 Paris, Cedex, France*

Received 6 December 2006; accepted 13 December 2006
Available online 27 December 2006

Abstract

Neutron vibrational spectroscopy measurements of $Pr_2Fe_{17}H_x$ and $Pr_2Fe_{17}D_x$ ($x \leq 5$) reveal dynamic features consistent with the interstitial hydrogen locations previously determined by neutron diffraction. In particular, for $Pr_2Fe_{17}H_3$, two peaks centered at ≈85.4 and 106.0 meV correspond to the normal-mode vibrational energies of hydrogen in octahedral (o) sites comprised of a near-square planar arrangement of four Fe atoms and two apical Pr atoms. Based on bond distances and preliminary first-principles calculations, the lower-energy feature is assigned to the H_o vibration along the *c*-oriented Fe—H_o—Fe axis. The higher-energy feature is assigned to the other two normal-mode H_o vibrations along the orthogonal Fe—H_o—Fe and Pr—H_o—Pr axes in the basal plane. For $Pr_2Fe_{17}H_4$ and $Pr_2Fe_{17}H_5$, the lower-energy H_o mode softens considerably by ≈6 and 10 meV, respectively. This is in part due to the *c*-axis expansion to accommodate the additional hydrogen occupying the neighboring distorted tetrahedral (t) sites comprised of two Fe atoms and two Pr atoms. For $Pr_2Fe_{17}H_5$, in addition to slightly softened H_o basal-plane modes centered at ≈104.7 meV, there is extra scattering intensity evident near ≈112 and 123.7 meV due to two of the H_t normal modes. The analogous $Pr_2Fe_{17}D_5$ spectrum suggests that the third H_t normal mode is located near 103.3 meV, obscured by the 104.7 meV H_o peak. A comparison of $Pr_2Fe_{17}H_x$ and $Pr_2Fe_{17}D_x$ vibrational energies indicates that the o-site bonding potential is largely harmonic, whereas the t-site bonding potential is more anharmonic.

Keywords: Interstitial alloys; Hydrogen storage materials; Magnetically ordered materials; Gas–solid reactions; Neutron scattering; Diffraction

1. Introduction

Hydrogen has a profound influence upon the structural and magnetic properties of the R_2Fe_{17} rare-earth (R) compounds. Typical of such compounds, Pr_2Fe_{17} crystallizes in the Th_2Zn_{17} rhombohedral ($R\bar{3}m$) structure. Hydrogen can insert into Pr_2Fe_{17} to form the hydrides $Pr_2Fe_{17}H_x$ ($0 \leq x \leq 5$) (see Fig. 1). Neutron diffraction results [1–3] indicate that the first three hydrogen atoms occupy the interstitial 9e distorted octahedral (o) sites, each comprised of four Fe atoms in a near-square planar configuration and two Pr atoms at the apices. Above $x = 3$, these o sites are completely filled, and the extra hydrogen atoms occupy up to one third of the available interstitial 18g tetrahedral (t) sites, each comprised of two Fe atoms and two Pr atoms at the corners. This is consistent with the fact that the lattice parameter *a* increases almost linearly with *x*, whereas the lattice parameter *c* remains unchanged up to $x = 3$ and then increases with further increases in *x* [3]. The t sites form arrays of isolated, partially hydrogen-occupied hexagons in the basal plane of the Pr_2Fe_{17} structure. The t-site hydrogen (H_t) atoms jump readily among adjacent vertices of each hexagon, as evidenced initially by Mössbauer spectroscopy [4] and subsequently in greater detail by quasielastic neutron scattering measurements [5,6]. This interesting H_t dynamical behavior is dictated by the details of the hydrogen binding potentials. To better understand these

* Corresponding author. Tel.: +1 301 975 6241; fax: +1 301 921 9847.
E-mail address: udovic@nist.gov (T.J. Udovic).
[1] Spallation Neutron Source, Oak Ridge National Laboratory, P.O. Box 2008, MS6475, Oak Ridge, TN 37831-6475, USA.

0925-8388/$ – see front matter © 2007 Elsevier B.V. All rights reserved.
doi:10.1016/j.jallcom.2006.12.084

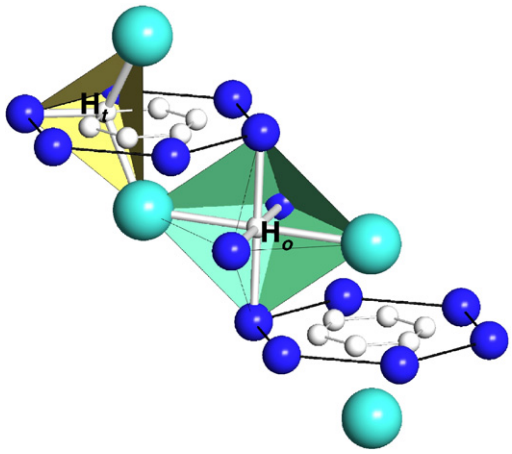

Fig. 1. Local surroundings of the H_o and H_t atoms in the crystal structure of the $Pr_2Fe_{17}H_x$ compounds. The large light, middle dark and small white spheres represent Pr, Fe and H atoms, respectively. H_o is centered in the shaded Fe_4Pr_2 octahedron. The hexagonal arrangements of H atoms indicate the six possible positions of H_t atoms per Fe hexagon. Only one shaded Fe_2Pr_2 tetrahedron with occupied H_t interstitial is presented for clarity. For $x = 3$, 4 and 5, there are zero, one and two such occupied H_t sites, respectively, per Fe hexagon.

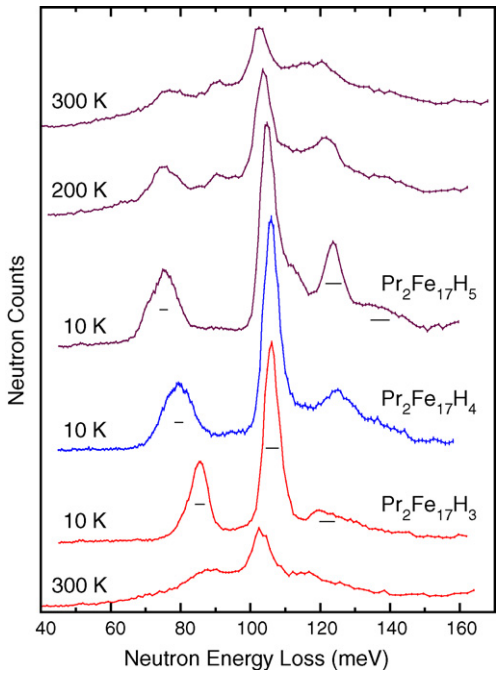

Fig. 2. Neutron vibrational spectra of $Pr_2Fe_{17}H_x$ ($x = 3$, 4, 5) at various temperatures. Spectra are normalized to the same Pr_2Fe_{17} mass and vertically offset for clarity.

potentials, we have performed neutron vibrational spectroscopy (NVS) measurements of both $Pr_2Fe_{17}H_x$ and $Pr_2Fe_{17}D_x$ ($x = 3$, 4, 5).

2. Experimental

Pr_2Fe_{17} samples were synthesized as reported previously [2]. Hydrogen and deuterium were loaded via gas-phase absorption. All neutron scattering measurements were performed at the NIST Center for Neutron Research. Samples were cooled with closed-cycle, He-refrigerated displexes. NVS measurements were performed with the Filter-Analyzer Neutron Spectrometer (FANS) [7] using the Cu(220) monochromator and horizontal collimations of either 40 or 20 min of arc before and either 20 or 10 min of arc after the monochromator. The resulting instrumental resolutions (full width at half maximum) are denoted by horizontal bars beneath the spectra. Lower-energy acoustic vibrational mode measurements (not shown here) were performed using the Fermi–Chopper time-of-flight spectrometer (FCS) [8] with an incident wavelength of 4.8 Å.

3. Results and discussion

Fig. 2 shows NV spectra for $Pr_2Fe_{17}H_x$ ($x = 3$, 4, 5). The $Pr_2Fe_{17}H_3$ spectra reflect the three normal-mode vibrations of the single type of interstitial o-site hydrogen (H_o). The relative intensities for the 10 K spectrum suggest that the lower-energy 85.4 meV feature reflects one mode and the higher-energy 106.0 meV feature reflects the other two. One of the high-energy modes was assigned to the H_o vibration along the basal-plane-oriented Fe–H_o–Fe axis, where the Fe–H_o bond distance is ≈1.89 Å [2]. This is consistent with the value of 105 meV found for the largely degenerate vibrational mode energy of octahedrally coordinated hydrogen in dhcp Fe hydride [9]. These o sites possess a local cubic symmetry with similar Fe–H_o bond distances of ≈1.894 Å [10]. Since the *c*-oriented Fe–H_o–Fe axis possesses a 0.1 Å longer Fe–H_o bond distance of ≈1.99 Å [2] than that along the basal-plane direction, the H_o vibration along this direction should be noticeably lower. Therefore, this vibration was assigned to the lower-energy 85.4 meV feature. By default, the remaining high-energy mode (near 106.0 meV) was assigned to the H_o vibration along the Pr–H_o–Pr axis. Given the Pr–H_o bond distances of 2.51 Å [2], this energy is somewhat higher than observed for analogous modes of octahedrally coordinated hydrogen in the β-phase rare-earth hydrides RH_{2+x} [11,12] with similar R–H_o bond distances [13]. We have initiated efforts to predict the phonon density of states for $Pr_2Fe_{17}H_x$ via first-principles phonon calculations based on density functional theory. Our preliminary results for $Pr_2Fe_{17}H_3$ corroborate the assignments described above, including the high energy of the H_o normal-mode vibration along the Pr–H_o–Pr axis.

Besides the main phonon features, the broad higher-energy band for $Pr_2Fe_{17}H_3$ centered at ≈120 meV is identified as an opto-acoustic multiphonon feature, typical in metal-hydride systems (*e.g.* [14]), and is associated with the combination of the 106.0 meV optical mode and a 14 meV acoustic mode band. Such an acoustic vibration peak has been experimentally observed in neutron energy gain at 150 K and above by FCS time-of-flight spectroscopic measurements. A similar multiphonon band 14 meV above the 85.4 meV peak is likely obscured by the presence of the main 106.0 meV peak. Comparing these results with the higher-hydride spectra in Fig. 2, the H_o vibration along the *c*-directed Fe–H_o–Fe axis shifts considerably lower by ≈6 meV (from 85.4 to 79.4 meV) for $Pr_2Fe_{17}H_4$ and by ≈10 meV (from 85.4 to 75.4 meV) for $Pr_2Fe_{17}H_5$. This is at least in part due to a lattice expansion along the *c* direction caused by the extra t-site hydrogens (H_t) (*i.e.* a 1.2% expansion upon going from $Pr_2Fe_{17}H_3$ to $Pr_2Fe_{17}H_5$ [3]). Yet, such a large relative shift may also reflect an H_t-induced perturbation of the H_o bonding potential. The existence and extent of such a perturbation will require more detailed *x*-dependent first-principles

calculations. Nonetheless, it seems likely that the addition of H_t atoms is responsible for the increased peak width evident for the lower-energy H_o mode, since the presence of H_t sublattice disorder [2,5] provides a distribution of H_t interactions with the H_o atoms.

In addition to the slightly softened, orthogonal H_o modes now maximized at ≈104.7 meV for $Pr_2Fe_{17}H_5$, the two new higher-energy vibrational features at ≈112 and 123.7 meV are assigned to two of the three expected H_t normal modes. The increased energies for these modes are consistent with the relatively smaller size of the t site compared to the o site, with Pr–H_t and Fe–H_t bond distances of 2.32 and 1.72 Å, respectively [2]. In β-PrH_2, for comparison, the H atoms reside in regular t sites with a slightly larger Pr–H_t bond distance of 2.38 Å, yielding an H_t normal-mode energy of 108 meV [15]. Unlike β-PrH_2, the presence of both Pr and Fe neighbors with different bond distances to H_t complicates the exact assignments of the observed H_t features in $Pr_2Fe_{17}H_5$. Such assignments will also require additional first-principles calculations. The relatively larger integrated intensity of the 104.7 meV H_o scattering band for $Pr_2Fe_{17}H_5$ compared with the corresponding band for $Pr_2Fe_{17}H_3$ at 10 K suggests that the third H_t normal-mode vibration is most likely located somewhere beneath this band. Our preliminary results from first-principles phonon calculations for $Pr_2Fe_{17}H_5$ are in qualitative agreement with the locations of the three H_t normal-mode vibrations and suggest that the two higher-energy modes are associated with H_t vibrations in the basal plane and the lowest-energy mode with out-of-plane H_t vibrations.

The 10 K $Pr_2Fe_{17}H_4$ spectrum in Fig. 2 also indicates the presence of H_t features but of lower intensity. Although the weaker lower-energy H_t feature is now more obscured by the surrounding H_o-related scattering bands, the more distinct higher-energy H_t peak displays a slight upshift to ≈125 meV, consistent with the somewhat smaller lattice constants at this hydrogen concentration compared to $Pr_2Fe_{17}H_5$ [3]. For both $Pr_2Fe_{17}H_4$ and $Pr_2Fe_{17}H_5$, broad multiphonon scattering is also evident ≈14 meV above the lowest-energy and highest-energy normal-mode peaks.

The $Pr_2Fe_{17}H_3$ and $Pr_2Fe_{17}H_5$ spectra at higher temperatures (200 and 300 K) in Fig. 2 reflect an attenuation of normal-mode intensities due to the temperature dependence of the significant Debye Waller factors for hydrogen. Moreover, the appearance of multiphonon bands also on the lower-energy side of the normal-mode peaks at these higher temperatures is due to opto-acoustic combinations involving 14 meV acoustic-mode de-excitations. The observed downward shift in the higher-energy H_o modes with increasing temperature is consistent with a temperature-induced lattice expansion. (*N.B.*, the 200 and 300 K spectra for $Pr_2Fe_{17}D_5$ in Fig. 3 indicate similar expected trends in peak attenuations and energy shifts as for $Pr_2Fe_{17}H_5$ upon increasing the temperature above 10 K.)

Fig. 3 shows NV spectra for $Pr_2Fe_{17}D_x$ ($x = 3, 4, 5$). Similar to the $Pr_2Fe_{17}H_3$ spectra, the $Pr_2Fe_{17}D_3$ spectrum reflects the vibrational peaks of interstitial o-site deuterium (D_o) at ≈60.0 and 75.1 meV, roughly scaled down by a harmonic factor of $1/\sqrt{2}$ with respect to those of the half-as-massive H_o atoms.

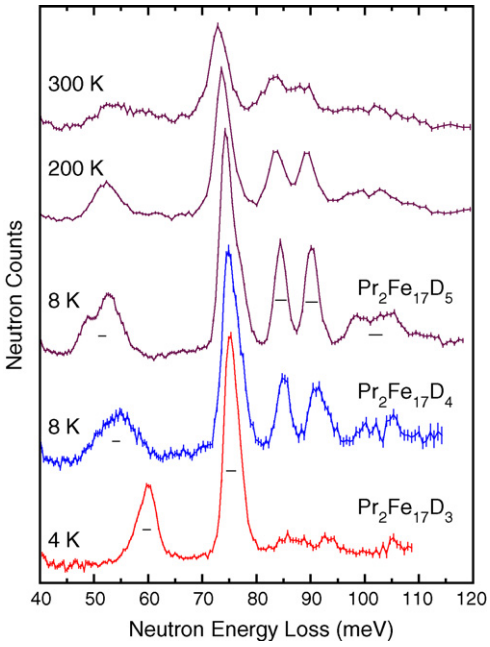

Fig. 3. Neutron vibrational spectra of $Pr_2Fe_{17}D_x$ ($x = 3, 4, 5$) at various temperatures. Spectra are normalized to the same Pr_2Fe_{17} mass and vertically offset for clarity.

For $Pr_2Fe_{17}D_4$ and $Pr_2Fe_{17}D_5$, there is a softening (analogous to $Pr_2Fe_{17}H_4$ and $Pr_2Fe_{17}H_5$) of the D_o vibrations with the appearance of t-site deuterium (D_t). Again, this softening is much more dramatic for the lower-energy mode, decreasing to ≈54.9 and 52.7 meV for $Pr_2Fe_{17}D_4$ and $Pr_2Fe_{17}D_5$, respectively. The corresponding higher-energy D_o mode decreases less dramatically to ≈74.9 and 74.2 meV, respectively. A more complex, broadened peak shape for the lower-energy D_o mode for $Pr_2Fe_{17}D_4$ and $Pr_2Fe_{17}D_5$ again suggests a distribution of force constants due to concentration-dependent D_t–D_o interactions originating from D_t sublattice disorder.

The D_t modes in Fig. 3 are evident at ≈84.4 and 90.1 meV for $Pr_2Fe_{17}D_5$ and at ≈85.0 and 91.0 meV for $Pr_2Fe_{17}D_4$. Unlike the largely harmonic o-site potential, these values reflect a t-site potential that is considerably anharmonic, with H/D normal-mode energy ratios of around 1.33 and 1.37 for the lower-energy and higher-energy modes, respectively. The contrast between o-site and t-site potentials is seen more clearly in the somewhat higher-resolution spectra in Fig. 4, where the ratio of energy-loss scales for $Pr_2Fe_{17}H_x$ and $Pr_2Fe_{17}D_x$ spectra is adjusted to equal the harmonic value of $\sqrt{2}$. It is interesting to note that a definite higher-energy shoulder near 77 meV emerges above the 74.2 meV D_o peak for $Pr_2Fe_{17}D_5$. This shoulder, which is absent from the 75.1 meV D_o peak for $Pr_2Fe_{17}D_3$ (see Fig. 3), is clear evidence of a third D_t normal-mode peak. A multipeak fit of this $D_o + D_t$ combined feature for $Pr_2Fe_{17}D_5$ places the D_t peak more precisely at 76.5 meV. Assuming an anharmonic H/D normal-mode energy ratio of 1.35 (the average for the other two observed D_t peaks) places the corresponding third H_t normal-mode energy for $Pr_2Fe_{17}H_5$ at ≈103.3 meV, which would indeed largely obscure it beneath the 104.7 meV H_o peak.

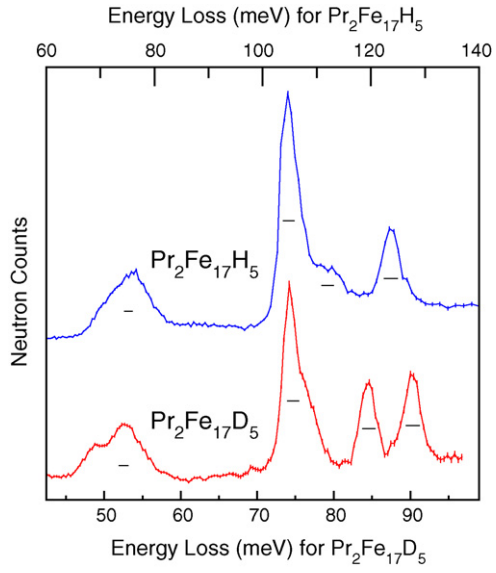

Fig. 4. Comparison of higher-resolution NV spectra for $Pr_2Fe_{17}H_5$ (10 K) and $Pr_2Fe_{17}D_5$ (8 K). The ratio of energy-loss scales for hydride and deuteride is equal to $\sqrt{2}$.

4. Summary

Neutron vibrational spectroscopy measurements of $Pr_2Fe_{17}H_x$ and $Pr_2Fe_{17}D_x$ ($x = 3$, 4, 5) have allowed assignment of the normal-mode vibrations of H and D in the octahedral and tetrahedral-type interstices. These results are consistent with the hydrogen locations determined from earlier diffraction results. A comparison of $Pr_2Fe_{17}H_x$ and $Pr_2Fe_{17}D_x$ vibrational energies indicates a largely harmonic o-site bonding potential, yet a considerably anharmonic t-site bonding potential. More thorough analyses of the hydrogen bonding potentials and their relationship to the rapid H_t hopping dynamics observed in this alloy await more detailed first-principles calculations.

References

[1] O. Isnard, S. Miraglia, J.L. Soubeyroux, D. Fruchart, A. Stergiou, J. Less-Common Met. 162 (1990) 273.
[2] O. Isnard, S. Miraglia, J.L. Soubeyroux, D. Fruchart, Solid State Commun. 81 (1992) 13.
[3] D. Hautot, G.J. Long, F. Grandjean, O. Isnard, S. Miraglia, J. Appl. Phys. 86 (1999) 2200.
[4] O. Isnard, S. Miraglia, J.L. Soubeyroux, D. Fruchart, P. L'Héritier, J. Magn. Magn. Mater. 137 (1994) 151.
[5] E. Mamontov, T.J. Udovic, O. Isnard, J.J. Rush, Phys. Rev. B 70 (2004) 214305.
[6] E. Mamontov, T.J. Udovic, J.J. Rush, O. Isnard, J. Alloys Compd. 422 (2006) 149.
[7] T.J. Udovic, D.A. Neumann, J. Leão, C.M. Brown, Nucl. Instrum. Methods Phys. Res. A 517 (2004) 189.
[8] J.R.D. Copley, T.J. Udovic, J. Res. Natl. Inst. Stand. Technol. 98 (1993) 71.
[9] K. Cornell, H. Wipf, V.E. Antonov, T.E. Antonova, A.I. Kolesnikov, E.G. Ponyatovsky, B. Dorner, Pol. J. Chem. 71 (1997) 1792.
[10] V.E. Antonov, K. Cornell, V.K. Fedotov, A.I. Kolesnikov, E.G. Ponyatovsky, V.I. Shiryaev, H. Wipf, J. Alloys Compd. 264 (1998) 214.
[11] T.J. Udovic, J.J. Rush, I.S. Anderson, J. Alloys Compd. 231 (1995) 138.
[12] T.J. Udovic, J.J. Rush, Q. Huang, I.S. Anderson, J. Alloys Compd. 253–254 (1997) 241.
[13] T.J. Udovic, Q. Huang, J.J. Rush, J. Alloys Compd. 356–357 (2003) 41.
[14] T.J. Udovic, J.J. Rush, I.S. Anderson, R.G. Barnes, Phys. Rev. B 41 (1990) 3460.
[15] D.G. Hunt, D.K. Ross, J. Less-Common Met. 49 (1976) 169.